Dalton Transactions

Accepted Manuscript

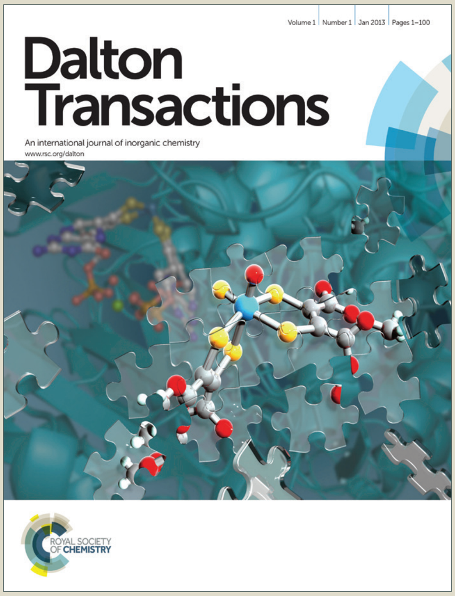

www.rsc.org/dalton

Table of contents entry

A family of novel Mn_3Ln_4 clusters: single-molecular magnets and first structurally characterized 3d/4f clusters containing 3-Methyloxysalicylaldoximate ligand

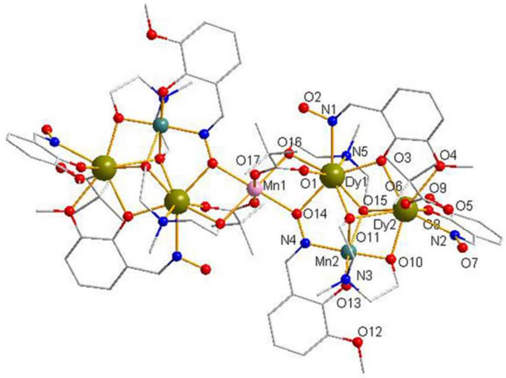

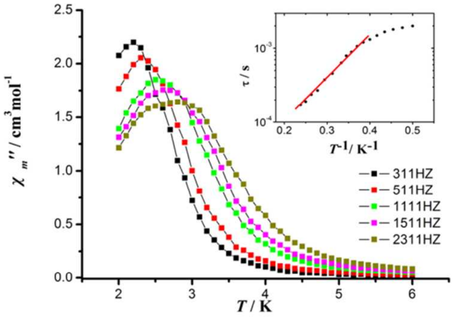

Cite this: DOI: 10.1039/c0xx00000x

www.rsc.org/xxxxxx

ARTICLE TYPE

Family of Novel Mn_3Ln_4 Clusters Displaying Single-Molecular Magnet Behavior

Hui Chen[a,b], Cheng-Bing Ma[a], Ming-Qiang Hu[a], Hui-Min Wen[a] and Chang-Neng Chen[a]*

Received (in XXX, XXX) Xth XXXXXXXXX 20XX, Accepted Xth XXXXXXXXX 20XX
DOI: 10.1039/b000000x

By using 3-Methyloxysalicylaldoxime (mosaoH_2) and N-methyl diethanolamine (N-mdeaH_2) as coligands, a family of heptanuclear Mn/Ln heterometallic compounds $[Mn^{II}Mn^{III}_2Ln^{III}_4(mosao)_2(mosaoH)_4(piv)_4(N\text{-}mdea)_4]\cdot xMeCN$ [Ln = Dy (**1**), Tb(**2**) and Y(**3**), pivH = pivalic acid] have been prepared. The crystal structures of **1**–**3** were obtained, and their core consists of two $Mn^{III}Ln_2(\mu_3\text{–}OR)_2$ (RO^{2-} = N-mdea^{2-}) triangles linked to a central Mn^{II} atom. Dc magnetic susceptibility study reveals that single-ion effects of the Ln ions are dominant in compounds **1** and **2**. As for compound **3**, which contains diamagnetic Y ions, the magnetic interactions between Mn ions via oximate NO bridges are revealed to be ferromagnetic. Fitting of the χ_mT vs T data gives g = 1.96 and J = 1.12 cm^{-1}, affording a $S = {}^{13}/_2$ ground state. All of the three compounds exhibit frequency-dependent out-of-phase ac susceptibility signals indicative of slow magnetization relaxation and potential SMM behavior. Among them, **1** and **3** display out-of-phase χ''_m peak maximum above 2.0 K. Fitting of the ac susceptibility data to an Arrhenius law gives energy barrier U_{eff} = 9.27/13.83 K for **1** and **3**, respectively.

Introduction

Single-molecule-magnets (SMMs) have drawn intense and continuing interests in recent years for their unique magnetic properties and potential applications in information storage or quantum computing.[1] SMMs are characterized as having a significant energy barrier to reversal of the magnetization vector, which originates from the combination of a large ground-state spin and a significant uniaxial (Ising) magnetic anisotropy, and thus can function as nanoscale magnets below a certain blocking temperature (T_B).[2] Since the discovery of the first SMM of $[Mn_{12}O_{12}(O_2CMe)_{16}(H_2O)_4]$ in 1993,[2b] the search for SMMs has been mainly focused on polynuclear 3d clusters,[3] and the majority of SMMs found are homometallic Mn clusters containing Mn^{III} atoms.[3a-f] Recently, the incorporation of lanthanide ions into such molecules as a promising route for probing new SMMs has attracted great interests owing to the significant single-ion anisotropy and a large ground-state spin of the lanthanide ions. An explosion of synthetic efforts has been devoted to 3d/4f clusters,[4] and several of them have been revealed to behave as SMMs.[4c-p] Among 3d/4f clusters, Mn/Ln based clusters are of particular interests due to the key role played by Mn^{III} ions as found in most of SMMs, and it is expected that combination of this two different high-spin and anisotropic metal ions will lead to SMMs with novel structures and desired magnetic properties, such as enhanced energy barriers. An increasing number of Mn/Ln heterometallic complexes with various nuclearities have been reported in recent years.[4e-h, 4p, 5] However, due to the synthetic difficulties in preparing Mn/Ln compounds that efforts toward mixed Mn/Ln compounds often resulted in all Mn or all Ln coordination compounds, the number of Mn/Ln based clusters is still limited. Thus, further examples of Mn/Ln clusters will provide valuable insights into the magnetic interactions, magneto-structural correlations and the favorable conditions for producing SMMs.

Phenolic oximes, such as salicylaldoxime (saoH_2) and its derivatives with their aldehydic hydrogen substituted by Me, Et, or Ph groups (R-saoH_2), have been widely employed in preparing polynuclear 3d complexes, especially Mn complexes, and is proved to be remarkably successful in mediation of ferromagnetic interactions between metal ions.[6] Recently, a few Mn/Ln clusters containing these ligands have been documented,[4f, 5f, 7] which exhibit fascinating magnetic properties, with a Mn_6Tb_2 cluster showing a high energy barrier of 103K.[4f] It is therefore of interest to extend families of Mn/Ln clusters of phenolic oximes and further examine the magneto-structural correlations within the families. 3-Methyloxysalicylaldoxime (mosaoH_2), as one kind of phenolic oxime which contains a methoxy group on 3–site of the aromatic ring in addition to the phenolic group and oximate group, has been less explored though. To the best of our knowledge, few polynuclear complexes with this ligand have been reported to date, except a tridecanuclear Co(II) cluster and two isostructural trinuclear Dy and Tb clusters.[8] Having the weakly coodinating methoxy group which may specifically bind to the Ln^{III} ions, as well as the phenolic group and oximate group, this multifunctional ligand can potentially coordinate to both 3d and

4f ions. Here, we present the first examples of 3d/4f polynuclear complexes containing mosaoH$_2$ ligand: [Mn^{II}Mn$^{III}_2$Ln$^{III}_4$(mosao)$_2$(mosaoH)$_4$(Piv)$_4$(N-mdea)$_4$] ·xMeCN [Ln = Dy (**1**), Tb(**2**) and Y(**3**)]. All of the three complexes exhibit slow magnetization relaxation.

Experimental section

Syntheses

All reagents are of commercially available analytical reagent grade and were used without further purification. [Mn$_3$O(piv)$_6$(py)$_3$] and mosaoH$_2$ were prepared according to the literature method. [8c, 9]

[Mn^{II}Mn$^{III}_2$Ln$^{III}_4$(mosao)$_2$(mosaoH)$_4$(Piv)$_4$(N-mdea)$_4$]·xMeCN. To a stirred colorless solution of mosaoH$_2$ (0.023g, 0.125mmol), [Mn$_3$O(piv)$_6$(py)$_3$] (0.026g, 0.025mmol) and Ln(NO$_3$)$_3$·6H$_2$O (0.125mmol) in MeCN (10mL) was added N-mdeaH$_2$ (0.16g, 0.13mmol) and NEt$_3$ (0.21mL, 1.5mmol). The resulting brown solution was stirred for 5 minutes and filtered. The filtrate was left undisturbed at room temperature for three days to deposit little prismatic black crystals in ～30% yield (based on Ln).

Anal. Calcd (found) for C$_{88}$H$_{126}$N$_{10}$O$_{34}$Mn$_3$Dy$_4$ (**1**) (solvent free): C,39.29 (38.94), H, 4.73 (5.02), N, 5.21 (4.93). Selected IR data (KBr, cm^{-1}): 3415(mb), 2957(w), 1617(w), 1560(s)，1483（m）,1458(s), 1438(m), 1422(m), 1362(w), 1325(w), 1279(m), 1242(m), 1220(m), 1107(w), 1065(s), 960(m), 885(w), 756(m), 740(m), 598(w).

Anal. Calcd (found) for C$_{88}$H$_{126}$N$_{10}$O$_{34}$Mn$_3$Tb$_4$ (**2**) (solvent free): C,39.61 (39.31), H, 4.76 (4.75), N, 5.25 (4.95). Selected IR data (KBr, cm^{-1}): 3413(mb), 2955(w), 1617(s), 1560(s)，1482（m）,1457(s), 1437(m), 1420(m), 1361(w), 1325(w), 1278(m), 1241(m), 1216(m), 1107(w), 1063(s), 958(m), 739(m), 597(w).

Anal. Calcd (found) for C$_{88}$H$_{126}$N$_{10}$O$_{34}$Mn$_3$Y$_4$ (**3**) (solvent free): C,44.25 (43.94), H, 5.32 (5.24), N, 5.86 (5.67). Selected IR data (KBr, cm^{-1}): 3419(mb), 2955(w), 1616(s), 1557(s)，1483（m）,1456(s), 1435(m), 1422(m), 1360(w), 1279(m), 1242(m), 1220(m), 1107(w), 1063(s), 959(m), 740(m), 597(w).

Physical measurements

Elemental analyses were carried out on a Vario EL III Elemental Analyzer. IR spectra were recorded on a Magna-75 FT-IR spectrometer using KBr pellets in the range of 4000 – 400 cm^{-1}. XRPD spectra were recorded on a MiniFlex II diffractometer at room temperature. Variable-temperature dc and ac susceptibility magnetic data for complexes **1**–**3** were measured on a PPMS-9T superconducting magnetometer employing the dried and finely ground polycrystalline samples kept in a capsule. Diamagnetic corrections were made with Pascal's constants for all the constituent atoms of the complexes.

X-ray Crystallography

X-ray single-crystal data of complexes **1**–**3** were collected on a Supernova diffractometer with Cu Kα radiation (λ = 1.5418 Å) using an ω-scan mode. Empirical absorption correction has been done using spherical harmonics, implemented in SCALE3 ABSPACK scaling algorithm. The structures were solved by direct methods and refined by full-matrix least-squares techniques using the SHELXTL-97 program package.[10] All non-hydrogen atoms were refined anisotropically. Hydrogen atoms were determined with geometrical calculations riding on the related atoms, and their positions and thermal parameters were fixed during structure refinement. The solvent molecules of complexes **1**–**3** are disordered and treated using the SQUEEZE option in PLATON.[11] Selected crystallographic data and refinement details for complexes **1** – **3** are displayed in Table 1.

Table 1. Selected crystallographic data and refinement details for **1**·3MeCN, **2**·6MeCN and **3**·4MeCN.

.	**1**·4MeCN	**2**·6MeCN	**3**·3MeCN
formula^a	C$_{96}$H$_{138}$Dy$_4$Mn$_3$N$_{14}$O$_{34}$	C$_{100}$H$_{144}$Tb$_4$Mn$_3$N$_{16}$O$_{34}$	C$_{94}$H$_{135}$Y$_4$Mn$_3$N$_{13}$O$_{34}$
fw, g mol^{-1}	2847.02	2914.81	2511.61
Cryst syst	triclinic	triclinic	triclinic
Space group	*P*-1	*P*-1	*P*-1
a, Å	12.5905(4)	12.5662(5)	12.5114(5)
b, Å	16.2570(6)	16.2692(8)	16.2168(9)
c, Å	16.7408(6)	16.7860(7)	16.7501(9)
α, deg	99.262(3)	65.082(4)	65.226(5)
β, deg	109.725(3)	70.517(4)	70.403(4)
γ , deg	112.780(3)	67.353(4)	67.618(4)
V, Å ^{3}	2801.02(17)	2811.5(2)	2790.0(2)
Z	1	1	1
T, K	100.0 (0)	100.0 (4)	100.0 (0)
ρ_{calcd}, g cm^{-3}	1.745	1.722	1.538
μ, mm^{-1}	17.379	15.464	6.045
F(000)	1471	1463	1329
$R_1{}^b$	0.0580	0.0632	0.0507
$wR_2{}^c$	0.1508	0.1659	0.1382

^{a} Including solvent molecules. ^{b} $R_1 = \sum(\,||F_o| - |F_c||\,) / \sum |F_o|$. ^{c} $wR_2 = [\sum w(F_o^2 - F_c^2)^2 / \sum w(F_o^2)^2]^{0.5}$.

Results and discussion

Synthesis

The use of performed small nuclearity species such as [Mn$_3$O]$^{n+}$, [Mn$_4$O$_2$]$^{n+}$, [Mn$_6$O$_2$]$^{n+}$ as starting materials in preparing Mn/Ln clusters has been proven to be successful.[4d, 4h, 4o, 5m, 12] Trimetallic clusters [Mn$_3$O]$^{n+}$ have been widely employed in preparing polynuclear Mn complexes and yielded fruitful products. However, there are only a few Mn/Ln clusters prepared from these compounds.[4l, 4o, 12-13] It is therefore of significance to further explore the potential of [Mn$_3$O] $^{n+}$ clusters as starting materials in Mn/Ln chemistry. In this work, we successfully obtained a family of novel Mn$_3$Ln$_4$ complexes by reaction of [Mn$_3$O(piv)$_6$(py)$_3$] with Ln(NO$_3$)$_3$·6H$_2$O, mosaoH$_2$ and N-mdeaH$_2$ in MeCN in the presence of NEt$_3$. The flexible multifunctional ligand N-mdeaH$_2$ was selected as an ancillary ligand considering the rigidity of the mosaoH$_2$ ligand. The first obtained compounds are **1** and **2**. As is known that an analogue containing a diamagnetic or an isotropic Ln ion will be of great help for the analysis of the magnetic behavior of families of isostructural 3d/4f complexes, Y^{III} and Gd^{III} analogues were attempted to prepare. However, only the Y^{III} analogue was obtained while the Gd^{III} analogue was failed to prepare despite the great efforts made for screening the suitable conditions. To find out if this reaction system could produce more complexes with various structures, a variety of reaction conditions concerning different solvent media and reagent ratios have also been explored. The slight modification of reagent ratios gave the same product with varying yields. However, replacing the solvent of MeCN by MeOH or DMF didn't afford any crystalline product, which is speculated that the generation of the complexes may be related with the polarity of the solvent.

Description of the crystal structures

The elemental analyses, IR spectra and XRPD data (Figure S1) indicate that the three complexes are isostructural. Crystal structures of **1**–**3** were pursued, and the structure of complex **1** is described here in detail as a representative.

The structure of complex **1** is presented in Figure 1 and selected interatomic distances and angles are listed in Table 2. Complex **1**·3MeCN crystallizes in the triclinic space group *P*-1. Central Mn1 is located on a crystallographic inversion center. Charge consideration, bond-valence-sum (BVS) calculation and the detection of Mn^{III} Jahn-Teller elongation axes indicate that Mn2 is trivalent, while Mn1 is in +2 oxidation state. The core consists of three Mn atoms and four Dy atoms arranged as two MnDy$_2$(μ_3–OR)$_2$ (RO^{2-} = N-mdea^{2-}) triangles linked to a central Mn1 atom through another pair of alkoxide O atoms of N-mdea^{2-} ligands. The metal atoms are additionally bridged by a pair of NO$^-$ oximate groups of doubly deprotonated mosao^{2-} ligands, two phenoxo O atoms of monodeprotonated mosaoH$^-$ ligands and two alkoxide O atoms of N-mdea^{2-} to give a complete [Mn$_2^{III}$Mn^{II}Dy$^{III}_4$(μ_3–OR)$_4$(μ–NO)$_2$(μ–OR)$_4$(μ–OR$'$)$_2$]$^{8+}$ core (R$'$O$^-$ = mosaoH$^-$) . Peripheral ligation is completed by two η^1: η^1: μ piv$^-$ ligands which bridge central Mn1 with adjacent Dy1 atoms, two monodentate coordinated piv$^-$ ligands and two chelating mosaoH$^-$ ligands on Dy2 atoms. As shown in Scheme 1, the mosao^{2-} ligands bridge in a η^1: η^1: η^2: μ_3 fashion and the mosaoH$^-$ ligands in a η^1: η^2: η^1: μ fashion. The N-mdea^{2-} ligands bridge in two different ways: two in a η^3: η^1: η^2: μ_4 ligation mode, two in a η^3: η^1: η^2: μ_3 ligation mode. All metal atoms are nearly located in one plane, with the largest deviation of 0.0351 Å provided by Mn2 and Mn2a atoms. The Mn-N-O-Dy torsion angle is 6.405°, and the Mn-N-O-Mn torsion angle is 5.081°. Each Mn atom is six coordinated with distorted octahedral geometry, and the Mn^{III} ions (Mn2 and Mn2a) exhibit John-Teller elongation with the axial bond distances of 2.1684 Å (Mn2-O15) and 2.2777 Å (Mn2-N3). The Dy atoms are eight coordinated to an O$_6$N$_2$ (Dy1) or O$_7$N$_1$ (Dy2) donor sets with a slightly distorted square-antiprismatic geometry. The distances between metal ions within the MnDy$_2$(μ_3–OR)$_2$ triangle range from 3.1907 Å to 3.5817 Å, and the distances between the central Mn1 atom and the adjacent atoms within triangle are 5.0511 Å (Mn1···Mn2) and 3.5491 Å (Mn1···Dy1). The structure of compounds **2** and **3** is very similar to that of **1**, except that Dy^{III} ions are replaced by Tb^{III} ions in **2** and Y^{III} ions in **3**. For compound **3**, the Mn-N-O-Mn torsion angle is 6.632°, and the distances between Mn ions are 5.0492 Å (Mn1···Mn2) and 10.0983 Å(Mn2···Mn2a).

To date, only a few heptanuclear Mn/Ln clusters have been reported, including the planar disc-like [Mn$_3$Ln$_4$],[5c] the bitetrahedral-to-triangle [Mn$_4$Dy$_3$][4p] and the [Mn$_4$Ln$_3$][14] clusters with a coaxial double-screw-propeller topology. Obviously, the core topology of compounds **1**–**3** is quite distinct from those of the above clusters. And compounds **1**–**3** represent the first structurally characterized 3d/4f clusters containing 3-methyloxysalicylaldoximate ligand.

Direct current magnetic susceptibility studies

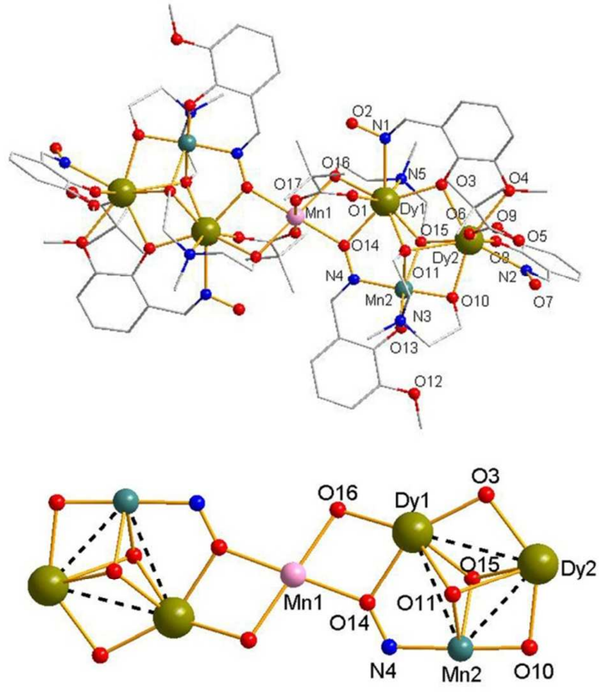

Figure 1. (top) Structure of compound **1**. (bottom) Representation of the complete [Mn$_2^{III}$Mn^{II}Dy$^{III}_4$(μ_3–OR)$_2$(μ–NO)$_2$(μ–OR)$_4$(μ–OR$'$)$_2$]$^{10+}$ core. Color scheme: Dy, green; Mn^{II}, pink; Mn^{III}, teal; O, red; N, blue; C, gray; Hydrogen atoms have been omitted for clarity.

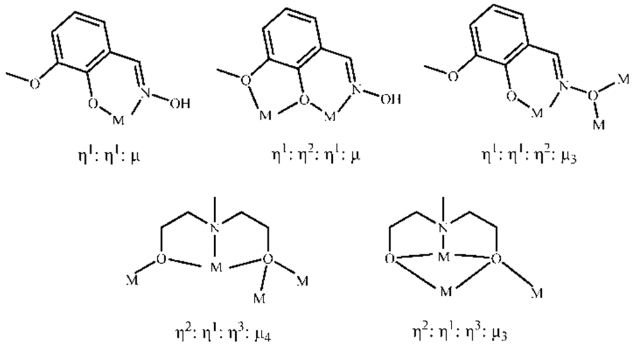

Scheme 1. The coordination modes of the mosao^{2-} ligand, mosaoH$^-$ ligand and N-mdea^{2-} ligand in compounds **1**–**3**.

The variable temperature dc magnetic susceptibility data for **1**–**3** were collected in the temperature range 2.0–300 K in an applied field of 0.1 T. Plots of χ_mT vs T for compounds **1**–**3** are shown in Figure 2. For **1**, the χ_mT value at 300K is 66.17 cm^3 Kmol^{-1}, close to the expected value of 67.07 cm^3 Kmol^{-1} for the uncoupled Mn$^{III}_2$Mn^{II}Dy$^{III}_4$ core (Dy^{III} : $S = {}^5/_2$, $L = 5$, $^6H_{15/2}$, $g = {}^4/_3$; Mn^{III}: $S = 2$, $g = 2$; Mn^{II}: $S = {}^5/_2$, $g = 2$). On lowering the temperature, the χ_mT product decreases steadily to 61.65 cm^3 Kmol^{-1} at 15K and then drops sharply to 43.08 cm^3 Kmol^{-1} at 2K. For **2**, the χ_mT value at 300K is 54.70 cm^3 Kmol^{-1}, slightly less than the expected value of 57.64 cm^3 Kmol^{-1} for the uncoupled Mn$^{III}_2$Mn^{II}Tb$^{III}_4$ core (Tb^{III} : $S = 3$, $L = 3$, $^7F_6$, $g = {}^3/_2$). The χ_mT value first decreases steadily with decreasing temperature to 51.43 cm^3 Kmol^{-1} at 18K, then increases to a maximum of 51.66 cm^3 Kmol^{-1} at 14.5K, and then down to 47.09 cm^3 Kmol^{-1} at 2K. The decrease in the χ_mT value for compounds **1** and **2** is mainly

Table 2. Selected interatomic distances (Å) and angles (deg) for complex **1**·4MeCN

Dy(2) ···Mn(2)	3.1907(14)	Dy(1) ···Mn(2)	3.4551(14)
Dy(2) ···Dy(1)	3.5818(8)	Dy(1) ···Mn(1)	3.5492(6)
Dy(2)-O(8)	2.178(7)	Dy(1)-O(1)	2.261(7)
Dy(2)-O(6)	2.271(6)	Dy(1)-O(3)	2.322(6)
Dy(2)-O(10)	2.302(7)	Dy(1)-O(15)	2.336(6)
Dy(2)-O(3)	2.379(6)	Dy(1)-O(14)	2.349(6)
Dy(2)-O(15)	2.395(6)	Dy(1)-O(16)	2.370(6)
Dy(2)-O(4)	2.461(6)	Dy(1)-O(11)	2.378(6)
Dy(2)-N(2)	2.491(9)	Dy(1)-N(1)	2.496(9)
Dy(2)-O(11)	2.608(6)	Dy(1)-N(5)	2.559(9)
Mn(1)-O(17)	2.171(7)	Mn(2)-O(13)	1.874(7)
Mn(1)-O(17)#1	2.171(7)	Mn(2)-O(10)	1.933(6)
Mn(1)-O(14)	2.185(6)	Mn(2)-O(11)	1.999(6)
Mn(1)-O(14)#1	2.185(6)	Mn(2)-N(4)	2.011(7)
Mn(1)-O(16)#1	2.195(7)	Mn(2)-O(15)	2.181(6)
Mn(1)-O(16)	2.195(7)	Mn(2)-N(3)	2.277(8)
Dy(1)-O(3)-Dy(2)	99.2(2)	Mn(2)-O(10)-Dy(2)	97.4(3)
Mn(2)-O(11)-Dy(1)	103.9(2)	Mn(2)-O(11)-Dy(2)	86.6(2)
Dy(1)-O(11)-Dy(2)	91.7(2)	Mn(1)-O(14)-Dy(1)	103.0(2)
Mn(2)-O(15)-Dy(1)	99.7(2)	Mn(2)-O(15)-Dy(2)	88.3(2)
Dy(1)-O(15)-Dy(2)	98.4(2)	Mn(1)-O(16)-Dy(1)	102.0(3)

#1: -x+2,-y+1,-z+1

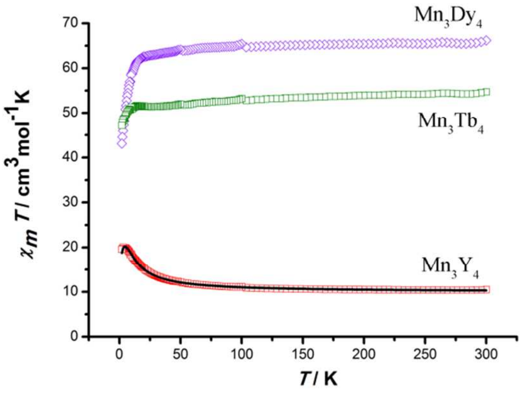

Figure 2. Plots of $\chi_m T$ vs T for compounds **1** – **3**. Solid line represents the best–fit curve using the parameters described in the text.

due to the thermal depopulation of the Stark sublevels arising from the crystal field splitting of the $^6H_{15/2}$ state for Dy^{III} ion and the $^7F_6$ state for Tb^{III} ion.[15] In a coupled system containing Ln ions coupled to transition–metal ions, the $\chi_m T$ value is related to both single–ion effect of the Ln ion and magnetic interactions between the spin carriers.[16] Consequently, the nature of the intramolecular global interactions for **1** and **2** could not be deduced unambiguously from the $\chi_m T$ versus T data in this case. For **3**, The $\chi_m T$ value at room temperature is 10.50 cm^3 Kmol^{-1}, close to the spin-only (g = 2) value of 10.38 cm^3 Kmol^{-1} for two S = 2 Mn^{III} and one $S = {}^5/_2$ Mn^{II} noninteracting ions, as Y^{III} ions are diamagnetic. Upon lowering the temperature, the $\chi_m T$ value increases continuously to 20.07 cm^3 Kmol^{-1} at 3K and then drops to 19.58 cm^3 Kmol^{-1} at 2K, which indicates a ferromagnetic interaction within the compound. The final decrease at the lowest temperatures is assigned to Zeeman effects, zero-field splitting, and/or weak intermolecular interactions.

The complexity of magnetic interactions and the presence of strongly anisotropic Dy^{III} and Tb^{III} ions preclude further analysis of pairwise interactions between metal ions in **1** and **2**. Thus, only susceptibility data of compound **3** containing diamagnetic Y^{III} ions have been simulated. In the compound, the Mn^{III} ion at each side is bridged to the central Mn^{II} ion through an oximate NO group, thus a linear trinuclear $S = 2 - {}^5/_2 - 2$ model based on the corresponding Hamiltonian [$\hat{H} = -2J(\hat{S}_1\hat{S}_2+\hat{S}_2\hat{S}_3)$] has been used, considering that the interactions between central Mn^{II} ion and the adjacent Mn^{III} ions are same and the interaction between two Mn^{III} ions is neglected (Mn^{III}···Mn^{III}, 10.0983 Å). In order to model the lowest temperature decrease of the $\chi_m T$ product, the mean field approximation was introduced for estimating intercluster interactions. Therefore, the following definition of susceptibility has been used:

$$\chi = \frac{\chi_{Mn_3}}{1 - \frac{ZJ'}{Ng^2{\mu_B}^2}\chi_{Mn_3}}$$

This model reproduces the experimental data well (Figure 2) and the best fit gives g = 1.95(8), J = 1.11(6) cm^{-1} and ZJ' = –0.01(0) K, affording a $S = {}^{13}/_2$ ground state. C. J. Milos, etc. have demonstrated that the exchanges within Mn_3 triangle through oximate groups are related with the individual Mn-O-N-Mn torsion angle and there is a *"magic area"* (30.4°-31.3°) for the torsion angles, less than 1° wide, above and below which they can predict the pairwise exchange to be ferro– or antiferromagnetic.[6b, 6f, 17] However, as for linear Mn_3 complexes via oximate bridges, several reports have revealed ferromagnetic interactions between Mn ions with the Mn-N-O-Mn torsion angles ranging from 2.54° to 51.3°.[5n, 18] In our study, although the Mn-N-O-Mn torsion angle in compound **3** is only 6.632°, the pairwise interaction of Mn ions is ferromagnetic, consistent with those found in the above mentioned studies.

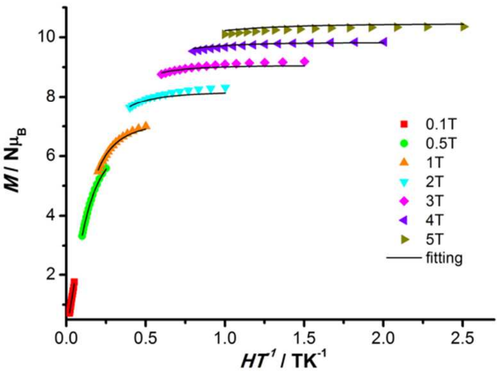

Figure 3. Plots of $M/N\mu_B$ vs H/T for compound **3** at the indicated applied fields. The solid lines represent the best fits of the data.

To investigate the anisotropy of the compounds and confirm the ground state of compound **3**, the magnetization data for compounds **1** – **3** were collected in the dc magnetic field range 0.1 – 5 T at 2.0 – 5.0 K and plotted as reduced magnetization $M/(N\mu_B)$ vs H/T in Figures S2, S3 and Figure 3. The data are not superimposed, indicating the presence of anisotropy and/or low-lying excited states in **1** – **3**. For **3,** which contains diamagnetic Y^{III} ions, the data were fitted using program ANISOFIT 2.0[19] by assuming only the spin ground state of the molecule is populated

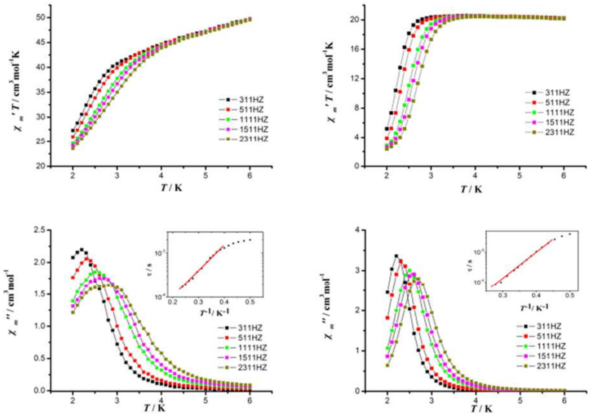

Figure 4. In-phase (shown as $\chi'_{\mathrm{m}}T$) and out-of-phase (χ''_{m}) ac susceptibility signals of compound **1** (left) and **3** (right) oscillating at the indicated frequencies at H_{ac} = 3.0G and H_{dc} = 0. Inset: the relaxation time τ versus T^{-1} plots; The solid lines represent the fits of the thermally activated region to the Arrhenius law.

and the spin Hamiltonian employed to fit is $\hat{H} = D\hat{S}_z^{\,2} + E(\hat{S}_x^{\,2} + \hat{S}_y^{\,2}) + g_{\mathrm{iso}}\mu_B S\cdot B$. The best fits are shown as the solid lines in Figure 3 with the parameters $S = {}^{13}/_2$, g = 1.85(9) and D = –0.46(2) cm^{-1}. Alternative fit with $S = {}^{11}/_2$ gave unreasonable values of g and D and thus was rejected. The lower-than-expected g value may be due to the inherent uncertainties in obtaining g from fits of bulk magnetization data and other experimental errors.[20] The M versus H curves at 2 K for **1** – **3** are shown in Figures S4-S6, **1** displays a hysteresis loop characteristic of a SMM, while **2** and **3** do not show sign of significant hysteresis effect.

Alternating current magnetic susceptibility studies

In order to probe the slow relaxation of magnetization, the ac susceptibility measurements were carried out on complexes **1**– **3** in the temperature range 2–15 K under a zero dc field and a 3.0 G ac field oscillating at five frequencies between 311 and 2311 Hz. All the three complexes display a frequency-dependent decrease in χ'_mT and concomitant appearance of out-of-phase χ''_m signals, indicating slow magnetic relaxation and potential SMM behavior (Figures 4 and S7). Compounds **1** and **3** display out-of-phase χ''_m peak maximum above 2.0 K, while the peaks of the χ''_m signals of compound **2** are located at temperatures well below 2.0 K. For each temperature, the relaxation time (τ) could be extracted from the fit of the corresponding out-of-phase χ''_m vs frequency (ω) data to generalized Debye model.[21] Then, the fit of the τ versus T^{-1} data of the thermally activated region to an Arrhenius law $\tau = \tau_0 \exp(U_{\mathrm{eff}}/k_{\mathrm{B}}T)$, where U_{eff} is the effective anisotropy energy barrier, k_{B} is the Boltzmann constant and τ_0 is the pre-exponential factor, gives $\tau_0 = 7.37\times10^{-6}/3.50\times10^{-7}$ s and energy barrier U_{eff} = 9.27/13.83 K for **1** and **3**, respectively. The Mydosh constants φ = (ΔTp/Tp)/(Δlog f) are 0.30 for **1** and 0.27 for **3**, comparable to those of other superparamagnets, which exclude the possibility of spin glass behavior (Figure. S8, S9). [22]

Since compound **3** exhibits a SMM behavior, it is concluded that slow relaxation could originate from the Mn ions solely. And in this case, the replacement of Y$^{\mathrm{III}}$ by Dy$^{\mathrm{III}}$ ions does not enhance the energy gap, which is different from those of other families of Mn/Ln clusters described in previous reports.[4h, 23] However, there are also some studies which demonstrate that the compounds with all metal ions of strong anisotropy do not achieve the highest SMM efficiency. For example, in the series of Co$^{\mathrm{II}}$ – Ln$^{\mathrm{III}}$ – Co$^{\mathrm{II}}$ linear trimetallic compounds, the isotropic Gd$^{\mathrm{III}}$ containing compound exhibits higher energy barrier compared to the Dy$^{\mathrm{III}}$ and Tb$^{\mathrm{III}}$ analogues.[24] And for the [Dy$_4$K$_2$] and [Dy$_5$]compounds, their diluted samples [DyY$_3$K$_2$] and [DyY$_4$], which contain only one Dy$^{\mathrm{III}}$ ion, exhibit more than 100K higher energy barrier than [Dy$_4$K$_2$] and [Dy$_5$].[25] The *ab initio* calculations have been used to understand this phenomenon.[25–26] In an exchange-coupled compound with strongly anisoptropic metal ions, the magnetic blocking is very complex as it involves both exchange and intraionic mechanisms and related to the number of relaxation paths available. U_{eff} as derived from the slope of the high-temperature ln(τ) versus T^{-1} data is often smaller than expected from calculated energies, resulting from a "short-cut" of the thermal barrier by quantum tunnelling of the magnetization (QTM). Therefore, the suppression of the quantum relaxation within the ground-state doublet or lower energy doublet will make the relaxation via higher excited states more competitive and thus increase the effective energy barrier. Conversely, it would decrease the effective energy barrier. In the system of Co$^{\mathrm{II}}$ – Ln$^{\mathrm{III}}$ – Co$^{\mathrm{II}}$, the suppression of QTM in Gd$^{\mathrm{III}}$ compound is much stronger than in the Dy$^{\mathrm{III}}$ and Tb$^{\mathrm{III}}$ analogues due to the multilevel blocking barriers in Gd$^{\mathrm{III}}$ analogue. The structure of blocking barriers of Gd$^{\mathrm{III}}$ compound consists of several excited states owing to the higher (8-fold) degeneracy of the ground-state multiplet on the Gd site, while it involves only one excited state in Dy and Tb analogues owing to the 2-fold degenerate ground-state manifolds on the Ln sites. And in compounds [Dy$_4$K$_2$] and [Dy$_5$], the intramolecular interactions between neighbouring Dy ions create significant local fluctuating transverse magnetic fields, which increase the tunnel splitting and make QTM relaxation via the ground-state doublet and the first excited doublet more competitive, thus reduce the experimental energy gap. It is suggested that similar situation is present in our case. Namely, the reduced suppression of QTM in Dy$^{\mathrm{III}}$ compound may be responsible for the lower effective energy barrier compared to Y$^{\mathrm{III}}$ analogue, which could originate from the reduced excited states levels of blocking barriers and/or the stronger transverse magnetic fields derived from the intramolecular interactions between neighbouring Dy$^{\mathrm{III}}$ and Mn$^{\mathrm{III}}$ ions.

Conclusions

Inspired by the remarkable success of phenolic oxime in mediation of ferromagnetic interactions between metal ions, we employed 3-methyloxysalicylaldoxime, a phenolic oxime derivatised ligand, to construct 3d/4f heterometallic clusters. A family of novel heptanuclear [Mn$_3$Ln$_4$] were obtained and structurally characterized. Their core consists of two Mn$^{\mathrm{III}}$Ln$^{\mathrm{III}}{}_2$(μ_3–OR)$_2$(RO^{2-} = N-mdea^{2-}) triangles linked to a central Mn$^{\mathrm{II}}$ atom. The compounds represent the first structurally characterized 3d/4f clusters containing 3-methyloxysalicylaldoximate ligand. Dc magnetic susceptibility study shows dominant single-ion effects of the Ln ions in compounds **1** and **2**. As for compound **3**, which contains diamagnetic Y$^{\mathrm{III}}$ ions, the magnetic interactions between Mn ions via oximate NO bridges are revealed to be ferromagnetic. Considering that the Mn-N-O-Mn torsion angle is only 6.632° in this work, it is suggested that the mediation of ferromagnetic or antiferromagnetic interactions via oximate groups in linear Mn_3 complex is not related with the Mn-N-O-Mn torsion angle as found in Mn_3 triangle motif. All of the three compounds exhibit frequency-dependent out-of-phase ac susceptibility signals indicative of slow magnetization relaxation and potential SMM behavior. The M versus H curve at 2 K for **1** displays a hysteresis loop.

Acknowledgement

This work was supported by the National Natural Science Foundation of China (Nos. 21173219, 21303201, 21203195 and 21101153).

Notes and references

[a] *State Key Laboratory of Structural Chemistry, Fujian Institute of Research on the Structure of Matter, The Chinese Academy of Sciences, Fuzhou, Fujian 350002, China. Fax: +86 591 83792395; E-mail: ccn@fjirsm.ac.cn*

[b] *University of Chinese Academy of Sciences, Beijing 100039, China.*

† Electronic Supplementary Information (ESI) available: [X-ray crystallographic data for complexes **1** – **3** in CIF format, Figures S1–S9. CCDC 1007481, 1017149 and 1007482]. See DOI: 10.1039/b000000x/

1. (a) R. Bagai and G. Christou, *Chem. Soc. Rev.*, 2009, **38**, 1011; (b) L. Bogani and W. Wernsdorfer, *Nat. Mater.*, 2008, **7**, 179; (c) G. Christou, D. Gatteschi, D. N. Hendrickson and R. Sessoli, *MRS Bull.*, 2000, **25**, 66; (d) M. N. Leuenberger and D. Loss, *Nature*, 2001, **410**, 789; (e) A. K. Powell, *Nat. Chem.*, 2010, **2**, 351; (f) D. Gatteschi, A. Caneschi, L. Pardi and R. Sessoli, *Science*, 1994, **265**, 1054.
2. (a) S. M. J. Aubin, N. R. Dilley, L. Pardi, J. Krzystek, M. W. Wemple, L. C. Brunel, M. B. Maple, G. Christou and D. N. Hendrickson, *J. Am. Chem. Soc.*, 1998, **120**, 4991; (b) R. Sessoli, D. Gatteschi, A. Caneschi and M. A. Novak, *Nature*, 1993, **365**, 141.
3. (a) T. C. Stamatatos, K. A. Abboud, W. Wernsdorfer and G. Christou, *Angew. Chem. Int. Ed.*, 2008, **47**, 6694; (b) M. H. Zeng, M. X. Yao, H. Liang, W. X. Zhang and X. M. Chen, *Angew. Chem. Int. Ed.*, 2007, **46**, 1832; (c) H. Miyasaka, R. Clerac, W. Wernsdorfer, L. Lecren, C. Bonhomme, K. Sugiura and M. Yamashita, *Angew. Chem. Int. Ed.*, 2004, **43**, 2801; (d) E. K. Brechin, M. Soler, J. Davidson, D. N. Hendrickson, S. Parsons and G. Christou, *Chem. Commun.*, 2002, 2252; (e) C. Boskovic, E. K. Brechin, W. E. Streib, K. Folting, J. C. Bollinger, D. N. Hendrickson and G. Christou, *J. Am. Chem. Soc.*, 2002, **124**, 3725; (f) A. J. Tasiopoulos, A. Vinslava, W. Wernsdorfer, K. A. Abboud and G. Christou, *Angew. Chem. Int. Ed.*, 2004, **43**, 2117; (g) H. Oshio, M. Nihei, S. Koizumi, T. Shiga, H. Nojiri, M. Nakano, N. Shirakawa and M. Akatsu, *J. Am. Chem. Soc.*, 2005, **127**, 4568; (h) C. Cadiou, M. Murrie, C. Paulsen, V. Villar, W. Wernsdorfer and R. E. P. Winpenny, *Chem. Commun.*, 2001, 2666; (i) H. Oshio, N. Hoshino and T. Ito, *J. Am. Chem. Soc.*, 2000, **122**, 12602; (j) S. L. Castro, Z. M. Sun, C. M. Grant, J. C. Bollinger, D. N. Hendrickson and G. Christou, *J. Am. Chem. Soc.*, 1998, **120**, 2365.
4. (a) M. Andruh, J. P. Costes, C. Diaz and S. Gao, *Inorg. Chem.*, 2009, **48**, 3342; (b) R. Sessoli and A. K. Powell, *Coord. Chem. Rev.*, 2009, **253**, 2328; (c) L.-F. Zou, L. Zhao, Y.-N. Guo, G.-M. Yu, Y. Guo, J. Tang and Y.-H. Li, *Chem. Commun.*, 2011, **47**, 8659; (d) V. Mereacre, Y. Lan, R. Clérac, A. M. Ako, W. Wernsdorfer, G. Buth, C. E. Anson and A. K. Powell, *Inorg. Chem.*, 2011, **50**, 12001; (e) J. L. Liu, F. S. Guo, Z. S. Meng, Y. Z. Zheng, J. D. Leng, M. L. Tong, L. Ungur, L. F. Chibotaru, K. J. Heroux and D. N. Hendrickson, *Chem. Sci.*, 2011, **2**, 1268; (f) M. Holynska, D. Premuzic, I.-R. Jeon, W. Wernsdorfer, R. Clerac and S. Dehnen, *Chem. Eur. J.*, 2011, **17**, 9605; (g) T. C. Stamatatos, S. J. Teat, W. Wernsdorfer and G. Christou, *Angew. Chem. Int. Ed.*, 2009, **48**, 521; (h) V. Mereacre, A. M. Ako, R. Clérac, W. Wernsdorfer, I. J. Hewitt, C. E. Anson and A. K. Powell, *Chem. Eur. J.*, 2008, **14**, 3577; (i) Y. F. Zeng, G. C. Xu, X. Hu, Z. Chen, X. H. Bu, S. Gao and E. C. Sanudo, *Inorg. Chem.*, 2010, **49**, 9734; (j) J. Rinck, G. Novitchi, W. Van den Heuvel, L. Ungur, Y. Lan, W. Wernsdorfer, C. E. Anson, L. F. Chibotaru and A. K. Powell, *Angew. Chem. Int. Ed.*, 2010, **49**, 7583; (k) A. M. Ako, V. Mereacre, R. Clerac, W. Wernsdorfer, I. J. Hewitt, C. E. Anson and A. K. Powell, *Chem. Commun.*, 2009, 544; (l) A. Mishra, W. Wernsdorfer, S. Parsons, G. Christou and E. K. Brechin, *Chem. Commun.*, 2005, 2086; (m) C. M. Zaleski, E. C. Depperman, J. W. Kampf, M. L. Kirk and V. L. Pecoraro, *Angew. Chem. Int. Ed.*, 2004, **43**, 3912; (n) S. Osa, T. Kido, N. Matsumoto, N. Re, A. Pochaba and J. Mrozinski, *J. Am. Chem. Soc.*, 2004, **126**, 420; (o) A. Mishra, W. Wernsdorfer, K. A. Abboud and G. Christou, *J. Am. Chem. Soc.*, 2004, **126**, 15648; (p) D. I. Alexandropoulos, T. N. Nguyen, L. Cunha-Silva, T. F. Zafiropoulos, A. Escuer, G. Christou and T. C. Stamatatos, *Inorg. Chem.*, 2013, **52**, 1179; (q) D. Dermitzaki, G. Lorusso, C. P. Raptopoulou, V. Psycharis, A. Escuer, M. Evangelisti, S. P. Perlepes and T. C. Stamatatos, *Inorg. Chem.*, 2013, **52**, 10235; (r) Z.-M. Zhang, L.-Y. Pan, W.-Q. Lin, J.-D. Leng, F.-S. Guo, Y.-C. Chen, J.-L. Liu and M.-L. Tong, *Chem. Commun.*, 2013, **49**, 8081.
5. (a) F. Cao, S. Wang, D. Li, S. Zeng, M. Niu, Y. Song and J. Dou, *Inorg. Chem.*, 2013, **52**, 10747; (b) J. Liu, C. Ma, H. Chen, M. Hu, H. Wen, H. Cui, X. Song and C. Chen, *Dalton Trans.*, 2013, **42**, 2423; (c) J. Liu, C. Ma, H. Chen, M. Hu, H. Wen, H. Cui and C. Chen, *Dalton Trans.*, 2013, **42**, 3787; (d) H. Chen, C.-B. Ma, M.-Q. Hu, H.-M. Wen, H.-H. Cui, J.-Y. Liu, X.-W. Song and C.-N. Chen, *Dalton Trans.*, 2013, **42**, 4908; (e) J.-L. Liu, W.-Q. Lin, Y.-C. Chen, J.-D. Leng, F.-S. Guo and M.-L. Tong, *Inorg. Chem.*, 2012, **52**, 457; (f) K. Hallier, M. Holynska, M. Rouzieres, R. Clerac and S. Dehnen, *Inorg. Chem.*, 2012, **51**, 3929; (g) Y. Zheng, X. J. Kong, L. S. Long, R. B. Huang and L. S. Zheng, *Dalton Trans.*, 2011, **40**, 4035; (h) A. Saha, M. Thompson, K. A. Abboud, W. Wernsdorfer and G. Christou, *Inorg. Chem.*, 2011, **50**, 10476; (i) C. Papatriantafyllopoulou, W. Wernsdorfer, K. A. Abboud and G. Christou, *Inorg. Chem.*, 2010, **50**, 421; (j) M. Y. Li, Y. H. Lan, A. M. Ako, W. Wernsdorfer, C. E. Anson, G. Buth, A. K. Powell, Z. M. Wang and S. Gao, *Inorg. Chem.*, 2010, **49**, 11587; (k) T. Shiga, T. Onuki, T. Matsumoto, H. Nojiri, G. N. Newton, N. Hoshino and H. Oshio, *Chem. Commun.*, 2009, 3568; (l) A. M. Ako, V. Mereacre, R. Clérac, I. J. Hewitt, Y. Lan, G. Buth, C. E. Anson and A. K. Powell, *Inorg. Chem.*, 2009, **48**, 6713; (m) V. M. Mereacre, A. M. Ako, R. Clerac, W. Wernsdorfer, G. Filoti, J. Bartolome, C. E. Anson and A. K. Powell, *J. Am. Chem. Soc.*, 2007, **129**, 9248; (n) C.-L. Zhou, Z.-M. Wang, B.-W. Wang and S. Gao, *Dalton Trans.*, 2012, **41**, 13620; (o) Z. Majeed, K. C. Mondal, G. E. Kostakis, Y. H. Lan, C. E. Anson and A. K. Powell, *Dalton Trans.*, 2010, **39**, 4740.
6. (a) A. G. Smith, P. A. Tasker and D. J. White, *Coord. Chem. Rev.*, 2003, **241**, 61; (b) R. Inglis, L. F. Jones, C. J. Milios, S. Datta, A. Collins, S. Parsons, W. Wernsdorfer, S. Hill, S. P. Perlepes, S. Piligkos and E. K. Brechin, *Dalton Trans.*, 2009, 3403; (c) C. I. Yang, W. Wernsdorfer, K. H. Cheng, M. Nakano, G. H. Lee and H. L. Tsai, *Inorg. Chem.*, 2008, **47**, 10184; (d) R. Inglis, L. F. Jones, G. Karotsis, A. Collins, S. Parsons, S. P. Perlepes, W. Wernsdorfer and E. K. Brechin, *Chem. Commun.*, 2008, 5924; (e) C. J. Milios, A. Vinslava, W. Wernsdorfer, S. Moggach, S. Parsons, S. P. Perlepes, G. Christou and E. K. Brechin, *J. Am. Chem. Soc.*, 2007, **129**, 2754; (f) C. J. Milios, R. Inglis, A. Vinslava, R. Bagai, W. Wernsdorfer, S. Parsons, S. P. Perlepes, G. Christou and E. K. Brechin, *J. Am. Chem. Soc.*, 2007, **129**, 12505.
7. G. Rigaux, R. Inglis, S. Morrison, A. Prescimone, C. Cadiou, M. Evangelisti and E. K. Brechin, *Dalton Trans.*, 2011, **40**, 4797.
8. (a) F.-S. Guo, J.-L. Liu, J.-D. Leng, Z.-S. Meng, Z.-J. Lin, M.-L. Tong, S. Gao, L. Ungur and L. F. Chibotaru, *Chem. Eur. J.*, 2011, **17**, 2458; (b) B.-W. Li, Y.-L. Zhou, Q. Chen and M.-H. Zeng, *Polyhedron*, 2010, **29**, 148; (c) I. J. Hewitt, Y. H. Lan, C. E. Anson, J. Luzon, R. Sessoli and A. K. Powell, *Chem. Commun.*, 2009, 6765.
9. R. Wu, M. Poyraz, F. E. Sowrey, C. E. Anson, S. Wocadlo, A. K. Powell, U. A. Jayasooriya, R. D. Cannon, T. Nakamoto, M. Katada and H. Sano, *Inorg. Chem.*, 1998, **37**, 1913.
10. G. M. Sheldrick, SHELXTL, 5.0, Siemens Analytical X-ray Instruments Inc., Madison, Wisconsin, USA, 1997.

11. P. Van der sluis and A. L. Spek, *Acta Crystallogr., Sect. A: Found. Crystallogr.*, 1990, **46**, 194.
12. A. Mishra, A. J. Tasiopoulos, W. Wernsdorfer, E. E. Moushi, B. Moulton, M. J. Zaworotko, K. A. Abboud and G. Christou, *Inorg. Chem.*, 2008, **47**, 4832.
13. (a) S. Mukherjee, M. R. Daniels, R. Bagai, K. A. Abboud, G. Christou and C. Lampropoulos, *Polyhedron*, 2010, **29**, 54; (b) A. Mishra, A. J. Tasiopoulos, W. Wernsdorfer, K. A. Abboud and G. Christou, *Inorg. Chem.*, 2007, **46**, 3105; (c) C. J. Milios, P. A. Wood, S. Parsons, D. Foguet-Albiol, C. Lampropoulos, G. Christou, S. P. Perlepes and E. K. Brechin, *Inorg. Chim. Acta*, 2007, **360**, 3932.
14. C. M. Liu, D. Q. Zhang and D. B. Zhu, *Dalton Trans.*, 2010, **39**.
15. J.-P. Sutter and M. L. Kahn, Lanthanide Ions in Molecular Exchange Coupled Systems. In *Magnetism: Molecules to Materials V*, Wiley-VCH Verlag GmbH & Co. KGaA: 2005; pp 161.
16. C. Benelli and D. Gatteschi, *Chem. Rev.*, 2002, **102**, 2369.
17. C. J. Milios, A. Vinslava, W. Wernsdorfer, A. Prescimone, P. A. Wood, S. Parsons, S. P. Perlepes, G. Christou and E. K. Brechin, *J. Am. Chem. Soc.*, 2007, **129**, 6547.
18. (a) M. Alexiou, C. Dendrinou-Samara, A. Karagianni, S. Biswas, C. M. Zaleski, J. Kampf, D. Yoder, J. E. Penner-Hahn, V. L. Pecoraro and D. P. Kessissoglou, *Inorg. Chem.*, 2003, **42**, 2185; (b) A. Audhya, M. Maity, S. M. T. Abtab, C. Mathonière, M. Kalisz and R. Clérac, *Polyhedron*, 2012, **33**, 353; (c) F. Birkelbach, U. Flörke, H.-J. Haupt, C. Butzlaff, A. X. Trautwein, K. Wieghardt and P. Chaudhuri, *Inorg. Chem.*, 1998, **37**, 2000; (d) T. Pathmalingam, S. I. Gorelsky, T. J. Burchell, A. C. Bedard, A. M. Beauchemin, R. Clerac and M. Murugesu, *Chem. Commun.*, 2008, 2782.
19. M. P. Shores, J. J. Sokol and J. R. Long, *J. Am. Chem. Soc.*, 2002, **124**, 2279.
20. (a) C. Lampropoulos, K. A. Abboud, T. C. Stamatatos and G. Christou, *Inorg. Chem.*, 2009, **48**, 813; (b) M. Murugesu, S. Takahashi, A. Wilson, K. A. Abboud, W. Wernsdorfer, S. Hill and G. Christou, *Inorg. Chem.*, 2008, **47**, 9459.
21. (a) K. S. Cole and R. H. Cole, *J. Chem. Phys.*, 1941, **9**, 341; (b) D. Gatteschi, R. Sessoli and J. Villain, in *Molecular Nanomagnets*, Oxford University Press Inc., New York, 2006.
22. J. A. Mydosh, in *Spin glasses:an experimental introduction*, Taylor & Francis, London Washington, DC, 1993.
23. (a) C. Papatriantafyllopoulou, K. A. Abboud and G. Christou, *Inorg. Chem.*, 2011, **50**, 8959; (b) V. Mereacre, M. N. Akhtar, Y. H. Lan, A. M. Ako, R. Clerac, C. E. Anson and A. K. Powell, *Dalton Trans.*, 2010, **39**, 4918.
24. (a) T. Yamaguchi, J.-P. Costes, Y. Kishima, M. Kojima, Y. Sunatsuki, N. Bréfuel, J.-P. Tuchagues, L. Vendier and W. Wernsdorfer, *Inorg. Chem.*, 2010, **49**, 9125; (b) V. Chandrasekhar, B. M. Pandian, J. J. Vittal and R. Clérac, *Inorg. Chem.*, 2009, **48**, 1148; (c) V. Chandrasekhar, B. M. Pandian, R. Azhakar, J. J. Vittal and R. Clerac, *Inorg. Chem.*, 2007, **46**, 5140.
25. R. J. Blagg, L. Ungur, F. Tuna, J. Speak, P. Comar, D. Collison, W. Wernsdorfer, E. J. L. McInnes, L. F. Chibotaru and R. E. P. Winpenny, *Nat. Chem.*, 2013, **5**, 673.
26. L. Ungur, M. Thewissen, J.-P. Costes, W. Wernsdorfer and L. F. Chibotaru, *Inorg. Chem.*, 2013, **52**, 6328.